Journal of Hydrology 578 (2019) 124082

Contents lists available at ScienceDirect

Journal of Hydrology

journal homepage: www.elsevier.com/locate/jhydrol

Research papers

Stochasting modeling of virus transport and removal during aquifer storage and recovery

Saeed Torkzaban[a,b,*], Mark Hocking[a], Scott A. Bradford[c], Sara S. Tazehkand[a,b], Salini Sasidharan[c,d], Jiří Šimůnek[d]

[a] Geological Survey of Victoria, PO Box 500, Melbourne, Victoria 3002, Australia
[b] National Centre for Groundwater Research and Training, Flinders University, Adelaide, SA 5001, Australia
[c] US Salinity Laboratory, USDA, ARS, Riverside, CA, USA
[d] Department of Environmental Sciences, University of California Riverside, Riverside, CA, USA

ARTICLE INFO

This manuscript was handled by Peter K. Kitanidis, Editor-in-Chief, with the assistance of Jian Luo, Associate Editor

Keywords:
Aquifer storage and recovery (ASR)
Virus attachment, detachment, and inactivation
Heterogeneous aquifers

ABSTRACT

A quantitative understanding of virus removal during aquifer storage and recovery (ASR) in physically and geochemically heterogeneous aquifers is needed to accurately assess human health risks from viral infections. A two-dimensional axisymmetric numerical model incorporating processes of virus attachment, detachment, and inactivation in aqueous and solid phases was developed to systematically evaluate the virus removal performance of ASR schemes. Physical heterogeneity was considered as either layered or randomly distributed hydraulic conductivities (with selected variance and horizontal correlation length). Geochemical heterogeneity in the aquifer was accounted for using Colloid Filtration Theory to predict the spatial distribution of attachment rate coefficient. Simulation results demonstrate that the combined effects of aquifer physical heterogeneity and spatial variability of attachment rate resulted in higher virus concentrations in the recovered water at the ASR well (i.e. reduced virus removal). While the sticking efficiency of viruses to aquifer sediments was found to significantly influence virus concentration in the recovered water, the solid phase inactivation under realistic field conditions combined with the duration of storage phase had a predominant influence on the overall virus removal. The relative importance of physical heterogeneity increased under physicochemical conditions that reduced virus removal (e.g. lower value of sticking efficiency or solid phase inactivation rate). This study provides valuable insight on site selection of ASR projects and an approach to optimize ASR operational parameters (e.g. storage time) for virus removal and to minimize costs associated with post-recovery treatment.

1. Introduction

Managed aquifer recharge (MAR) is increasingly used worldwide to replenish aquifers to meet growing demands for a secure and sustainable supply of potable and non-potable water. MAR is a broad term for a variety of methods of recharging and recovering water from aquifers. For example, one of the most common types of MAR is the Aquifer Storage and Recovery (ASR) technique (Page et al., 2016) which injects and recovers water via the same well. A variety of water types such as stormwater runoff and secondary treated wastewater can be used as source water in ASR schemes. The source water (e.g., urban stormwater) is usually contaminated with pathogenic microbes such as viruses, bacteria, and protozoa. Viruses are generally designated as the microbial pathogen of greatest risk because of their low infectious dose and potential to travel long distances in aquifers (Reynolds et al., 2008). Several studies have reported that viruses can travel several hundred meters or may be viable for several months (or even years) under certain environmental conditions (Sidhu et al., 2015; Torkzaban et al., 2006; Schijven et al., 2016). The potential for large transport distance and long-term survival for pathogenic viruses in aquifers is a significant public health concern. Indeed, one of the main impediments to the uptake of ASR has been attributed to the presence of pathogenic viruses in the recovered water (NRMMC-EPHC-NHMRC, 2009). Recovered ASR water is therefore subjected to expensive post-treatments to remove/inactivate pathogens (Dillon et al., 2010).

Schijven and Hassanizadeh (2000) presented a comprehensive review on factors and processes influencing virus removal in laboratory and field studies. Processes influencing virus transport and removal in aquifers include advective and dispersive transport, attachment to and detachment from sediment surfaces, and inactivation in aqueous and on

* Corresponding author at: Geological Survey of Victoria, PO Box 500, Melbourne, Victoria 3002, Australia.
E-mail address: saeed.torkzaban@ecodev.vic.gov.au (S. Torkzaban).

https://doi.org/10.1016/j.jhydrol.2019.124082
Received 19 June 2019; Received in revised form 21 August 2019; Accepted 26 August 2019
Available online 27 August 2019

solid phases (Sasidharan et al., 2018; Anders and Chrysikopoulos, 2005). In addition, previous research suggests that physical and geochemical heterogeneities of the aquifer play an important role in the process of microbial transport and removal (Bhattacharjee et al., 2002; Maxwell et al., 2007; Rehmann et al., 1999; Katzourakis and Chrysikopoulos, 2018). For example, preferential flow paths, such as fractures or regions with high hydraulic conductivity, in a physically heterogeneous aquifer are recognized to significantly increase the transport of contaminants and microbial pathogens in aquifers (Masciopinto et al., 2008; Bradford et al., 2017). Accurate predictions of virus removal during ASR, therefore, require consideration of removal factors and aquifer heterogeneity. These predictions can then be used to evaluate the suitability of the recovered water for its intended use and to determine the required degree of post-recovery treatment.

Aquifers are known to be physically and geochemically heterogeneous (Harvey et al., 1993, Kitanidis, 1997; Dagan et al., 2003). Poor characterization of aquifer heterogeneity is an important factor that hampers accurate predictions of both flow and contaminant transport. In contrast to homogeneous conditions, aquifer heterogeneity is expected to produce irregular concentration fronts with enhanced virus transport in certain parts of the aquifer. The last two decades have seen the development of a relatively large number of models that predict flow and solute transport in heterogeneous porous media (Jarvis and Larsbo, 2012; Šimůnek et al., 2003; Wang et al., 2014). However, most microbial modeling studies reported in the literature have only dealt with homogeneous porous media (Anders and Chrysikopoulos, 2005; Jin and Flury, 2002; Rockhold et al., 2004; Unc and Goss, 2004). Relatively speaking, there are fewer studies that have considered the effect of physical and chemical aquifer heterogeneity on virus transport and removal (Hornstra et al., 2018; Bhattacharjee et al., 2002; Pang, 2009; Sinreich and Flynn, 2011). Recently, Katzourakis and Chrysikopoulos (2018) extensively investigated the effect of spatially variable attachment coefficient on biocolloid transport in geochemically heterogeneous porous formations and suggested that neglecting to account for aquifer chemical heterogeneity may lead to erroneous predictions of virus transport in porous media. To date, the effect of aquifer heterogeneity on the virus removal performance during ASR, in which injection and recovery occur from the same well, has not yet been studied.

Few ASR field experiments have been conducted to investigate virus removal because they are expensive, time-consuming, and experimentally challenging (Sidhu et al., 2015). Nonetheless, several laboratory and field studies using bacterial viruses as surrogates for human viruses during aquifer recharge have yielded significant insight into the processes of virus transport and removal during ASR. For example, virus attachment rates appear to be faster than detachment rates in field studies (Bales et al., 1997; Schijven et al., 1999, Schijven and Hassanizadeh, 2000, Anders and Chrysikopoulos, 2005, Hornstra et al., 2018). Several lab studies have shown that virus inactivation rate is much greater when they are attached on mineral surfaces than in free water (Hsu et al., 2011; Sasidharan et al., 2018). In contrast, several other studies reported that mineral surfaces such as quartz sand and clay-sized particles offered protection against virus inactivation under certain conditions (Anders and Chrysikopoulos, 2006; Chrysikopoulos and Aravantinou, 2012). Consequently, the relative importance of solid phase inactivation remains a controversial (or perhaps case-specific) issue. Recently, Sasidharan et al. (2018) reported that virus removal by attachment and solid phase inactivation may be enhanced by adjusting the storage time in the ASR operation. However, no studies have systematically investigated the influence of storage time on the removal of viruses due to attachment and solid phase inactivation of viruses during ASR.

In this paper, we have developed a two-dimensional axisymmetric virus transport model to assess the removal of viruses in an ASR scheme under various operational conditions. In this model, aquifer heterogeneity is considered either as layered or random distributions of hydraulic conductivity with various standard deviations and correlation lengths. The virus transport equation is coupled with the fluid flow equation. The model is used to perform a systematic investigation on the influence of virus removal parameters (attachment, detachment, and solid and aqueous phase inactivation), physical and chemical aquifer heterogeneity, and storage time on virus removal during ASR. We show that the incorporation of aquifer heterogeneity into the transport model results in predictions which are significantly different than those obtained from models developed for homogeneous aquifers.

2. Materials and method

2.1. Governing equations

We assumed an ASR system with a fully penetrated pumping well installed in a confined aquifer. The three-dimensional domain was modeled using a two-dimensional axisymmetric cross-section. The vertical axis of rotation was located at the pumping well (herein referred to as the ASR well). An ASR cycle consisted of an injection, storage, and recovery phase. The groundwater velocity was assumed to be at steady-state during each phase and the transition period between two phases was neglected. Furthermore, the effect of flow reversal during the recovery phase on mobilization of attached viruses was neglected based on available results in the literature (Sasidharan et al., 2018). During the injection phase, water with a constant virus concentration was injected into the aquifer and a concentration front moved away from the ASR well. During the recovery phase, stored water was extracted via the same ASR well and the concentration front moved toward the well. For simplicity, we assume that the injection and recovery flow rates were the same and the effect of regional groundwater flow was not considered during these phases. Our axisymmetric model does not allow the simulation of non-symmetric conditions such as regional groundwater flow. Modelling virus transport in an ASR scheme with a regional hydraulic gradient requires a 3-dimensional model which introduces extra variables and complicates the investigation. In this paper, we have sought to understand the fundamental removal processes of viruses in ASR systems in which the average water velocity during injection and recovery phases is significantly greater than the native groundwater velocity. However, to study virus removal during storage phase, the water velocity was determined based on a regional hydraulic gradient of 0.001 to estimate the attachment rate coefficient (to be discussed later).

The governing equation for the two-dimensional, axisymmetric, and transient water flow in a heterogeneous confined aquifer is as follows (Schijven et al., 2010):

$$S_s \frac{\partial h}{\partial t} = \frac{\partial}{\partial z}\left(k_z \frac{\partial h}{\partial z}\right) + \frac{1}{r}\frac{\partial}{\partial r}\left(k_r r \frac{\partial h}{\partial r}\right) \quad (1)$$

where h [L, where L denotes units of length] is the hydraulic head, t [T, where T denotes units of time] is the time, S_s [L^{-1}] is the specific storage, and k_z and k_r [$L\,T^{-1}$] are the hydraulic conductivity in the z (vertical) and r (radial) [L] directions. The spatially distributed hydraulic heads were determined and then used to calculate the water velocity by applying Darcy's law as $v_r = (-k_r/n)(\partial h/\partial r)$ and $v_z = (-k_z/n)(\partial h/\partial z)$ where v_r [$L\,T^{-1}$] and v_z [$L\,T^{-1}$] are the vertical and radial pore water velocities, respectively, with porosity denoted by n [–].

Virus transport in the aquifer was described using the advection–dispersion equation along with appropriate terms for virus attachment, detachment, and inactivation:

$$\frac{\partial C^*}{\partial t} + \frac{\partial S^*}{\partial t} = D_{zz}\frac{\partial^2 C^*}{\partial z^2} + \frac{1}{r}\frac{\partial}{\partial r}\left(D_{rr} r \frac{\partial C^*}{\partial r}\right) - v_z \frac{\partial C^*}{\partial z} - v_r \frac{\partial C^*}{\partial r} - Q$$

$$Q = \mu_l C^* + \mu_s S^* \quad (2)$$

$$\frac{\partial S^*}{\partial t} = K_{att} C^* - K_{det} S^* - \mu_s S^*$$

where C^* is the normalized virus concentration defined as C/C_{in} (where C_{in} [N L^{-3}] is the number [N] of virus per unit volume in water during the injection phase), S^* is the normalized adsorbed virus concentration defined as $S^* = \frac{\rho_b S}{n C_{in}}$ (S [N M^{-1}] is the number of attached viruses per unit mass [M] of sediment and ρ_b [M L^{-3}] is the bulk density of the sediment), μ_l and μ_s [T^{-1}] are the inactivation rate coefficients for the free viruses and attached viruses, respectively, and K_{att} and K_{det} [T^{-1}] are rate constants for virus attachment and detachment, respectively, that will be described later. Finally, D_{zz} and D_{rr} [L^2 T^{-1}] are the dispersion coefficients in z and r directions, given by:

$$D_{zz} = \alpha_z |v| + D_{diff} + (\alpha_r - \alpha_z)\frac{v_z v_z}{|v|}$$
$$D_{rr} = \alpha_z |v| + D_{diff} + (\alpha_r - \alpha_z)\frac{v_r v_r}{|v|} \quad (3)$$

where α_z and α_z [L] are the vertical and radial dispersivities, $|v|$ [L T^{-1}] is the velocity magnitude and D_{diff} [L^2 T^{-1}] is the molecular diffusion coefficient.

2.2. Model parameters

Table 1 shows the baseline flow and transport parameters used in the simulations. The ranges of these parameters, typically estimated in laboratory and field studies, are also listed in the table. All simulations were conducted using parameter values that lie within the specified ranges. Even in cases of randomly heterogeneous conditions, the hydraulic conductivity and geochemical distributions were determined such that the specified ranges of these heterogeneities were never exceeded.

For our modeling purposes, attachment and detachment were modeled as first-order processes. According to the Colloid Filtration Theory (CFT), the attachment coefficient is assumed to be related to the average flow velocity as (Yao et al., 1971):

$$K_{att} = \frac{3}{2}\frac{(1-n)}{d_{50}}\alpha\eta v \quad (4)$$

where d_{50} [L] is the median grain size, α [−] is the sticking efficiency and η [−] is the single-collector contact efficiency representing the ratio of the number of particles approaching the collector to the number of particles striking a collector. A correlation equation developed by Messina et al. (2015) was used to calculate η as a function of parameters such as Peclet number, grain size, virus size, and virus density (1.05 g cm^{-3}). This recently developed equation provides η values lower than one over a wide range of parameters and it is valid for virus-size particles. The sticking efficiency parameter (α) is defined as the ratio of the number of collisions that result in attachment to the total number of collisions (Tufenkji and Elimelech, 2004). Essentially, the value of α represents the probability that a collision will succeed in attachment. The significance of the sticking efficiency is that, in contrast to K_{att}, it is considered to be independent of flow velocity.

Table 1
Hydrologic and transport parameters used in the model simulations.

Parameter	Basic value	Comments
Well radius	0.1 m	
Aquifer thickness	20 m	
Anisotropy ration (r:z)	1	
Injection and recovery rates	300 m^3 day^{-1}	100–1000
Hydraulic conductivity, K	5 m day^{-1}	0.1–100
Specific storage, S_s	1×10^{-5} m^{-1}	
Dispersity (longitudinal), α_r	0.1 m	
Dispersity (transverse), α_z	0.01 m	
Porosity, n	0.4	
Transport Parameters		
Median grain diameter, d_{50}	2.5×10^{-4} m	
Virus diameter, d_p	5.0×10^{-8} m	
Sticking efficiency, α	1×10^{-3}	0–1×10^{-2}
Detachment rate coefficient, K_{det}	0.001 day^{-1}	0–0.1 day^{-1}
Aqueous inactivation rate coefficient, μ_l	0.01 day^{-1}	0–0.1 day^{-1}
Solid phase inactivation rate coefficient, μ_s	0.05 day^{-1}	0–0.1 day^{-1}

In this study, the representative sediment grain size was taken to be d_{10} [L] (Bradford et al., 2017) i.e., where 10% of the sediment mass is finer than d_{10}. The value of d_{10} was related to the hydraulic conductivity (K) distribution using the Kozeny–Carman equation (Bear, 1972) as:

$$d_{10} = \left(\frac{K X_w}{\rho_w g}\frac{180(1-n)^2}{n^3}\right)^{0.5} \quad (5)$$

where ρ_w [M L^{-3}] is the density of water, X_w [M L^{-1} T^{-1}] is the dynamic viscosity of water, and g [L T^{-2}] is the acceleration due to gravity. Note that $d_{50} = d_{10}U_i$, where U_i is the uniformity coefficient that was taken to be 4. The use of Eq. (5) in this manner allowed d_{50} in CFT calculations to be related to K.

2.3. Physical heterogeneity of aquifer

Spatial variations in the hydraulic conductivity result in a heterogeneous flow field that influences virus transport and the concentration distribution in the aquifer. Two types of physical heterogeneity were investigated: layered and random heterogeneities. In a layered system, the aquifer was divided into three layers with separate hydraulic conductivities. Aquifers with fractures, large blocks of macro-pores, or various sedimentary deposits may be described as a layered aquifer (Ibaraki and Sudicky, 1995).

Evidence from field-scale hydraulic conductivity measurements indicates that the spatial distribution of hydraulic conductivity is log-normally distributed (Sudicky and MacQuarrie, 1989). Indeed, Freeze (1975) pointed out that the lognormal distribution of K typically has a standard deviation (in log base 10 units) ranging from 0.2 to 2.0. In this study, we employed the HYDRUS (2D/3D) computer software (Simunek et al., 2016) to generate stochastic (random) distributions of hydraulic conductivity scaling factor. HYDRUS uses the spectral approach of Mejia and Rodriguez-Iturbe (1974) which is based on an auto-correlated log-normal distribution. Using this method, a specific K value can be assigned to the flow domain that is then multiplied in each node by a scaling factor (λ). The stochastic distribution requires three input parameters: the standard deviation (σ) of log10(λ), and its correlation length in the lateral (the X-correlation length) and vertical (the Z-correlation length) directions. The value of σ determines the extent of variations in the scaling factors, with higher values leading to higher variations in scaling factors. On the other hand, the correlation length is a measure of the distance in a specific direction that scaling factors are related. A high value of the X-correlation length means that the scaling factor maintains similar values for a greater horizontal distance. In this study, various combinations of σ and lateral correlation length were considered.

2.4. Correlation of the sticking efficiency with the hydraulic conductivity

A randomly distributed K leads to spatial variations of the pore water velocity and d_{10} as described by Eqs. (1) and (5). Moreover, the parameter α in Eq. (4) was assumed to be correlated with K. Consequently, spatial variability in K produced random values of K_{att}. Unlike the grain size parameter (d_{50}), there are no established empirical expressions relating the value of α to K. The empirical approach of Garabedian et al. (1988) was therefore employed to relate α to K as:

$$\ln(\alpha) = \ln(\bar{\alpha}) + \omega \ln(K) \quad (6)$$

where ω is the correlation coefficient and $\bar{\alpha}$ represents the portion of

the sticking efficiency that depends on solution (e.g., pH and ionic strength), sediment (e.g., metal oxide content), and virus properties (e.g., surface properties) that cannot be accounted for by variability in the K field. Therefore, the effects of variability of solution, sediment, and virus properties were not directly considered and were beyond the scope of this paper. Using this approach, it is possible for the value of α to be positively correlated to K ($\omega > 0$), negatively correlated to K ($\omega < 0$), or uncorrelated to K ($\omega = 0$). Note that in case of a constant value of α the variability of K_{att} only occurs through spatial variability of d_{50} and ν using Eq. (4). In an aquifer with randomly distributed heterogeneities, we assumed ($\omega < 0$) because previous research found that the value of α was higher in a low-conductivity than in a high-conductivity porous media (Harvey et al., 1993; Morley et al., 1998). This finding was attributed to the presence of iron-rich coatings, minerals which were most abundant in the finer-grained sediments, leading to greater colloid sticking efficiencies. The value of ω was chosen as -0.1. The value of $\bar{\alpha}$ was chosen to range between 10^{-5} for highly unfavorable attachment conditions (e.g. anoxic conditions) to 10^{-2} for modestly favorable conditions reported for limestone aquifer (Sasidharan et al., 2017). For the simulations performed in this paper, detachment was assumed to be uncorrelated with K as there is no established empirical expression in the literature relating the value of K_{det} to K.

Several virus transport models have been developed that incorporate constant first-order inactivation of free (μ_l) and attached (μ_s) viruses (Chrysikopoulos and Sim, 1996; Sim and Chrysikopoulos, 1996). Based on the existence two or more subpopulations of viruses in a suspension with different inactivation rate coefficients, Sim and Chrysikopoulos (1996) also developed a transport model, incorporating kinetic reversible adsorption and different time-dependent inactivation rate coefficients for suspended and attached viruses. This more sophisticated way of modeling virus inactivation during subsurface transport under saturated conditions may also be useful when considering heterogeneous populations of different viruses that exhibit multiphasic inactivation. However, in this study, we modelled virus inactivation as a first-order decay process with different rate coefficients for free and attached viruses. Literature data show that inactivation rate coefficients of viruses in the solution phase range between 0.005 and 0.1 day^{-1}, depending on the temperature and virus type (Sidhu et al., 2015, Hornstra et al., 2018). In our simulations, the solution-phase inactivation coefficient was set to 0.01 day^{-1}. For surface inactivation, the values of μ_s were chosen to range from 0 to 0.1 day^{-1}. Recent research has shown that values of μ_s for bacteriophages PRD1 and ΦX174 were several orders of magnitude greater than μ_l (Sasidharan et al., 2018). Bacteriophages MS2, PRD1 and ΦX174 are commonly used as surrogates to human viruses (Schijven and Hassanizadeh, 2000). However, recent experimental studies with real pathogenic enteric viruses (adenovirus) have reported that the attachment behavior of surrogate phages MS2 and ΦX174 is substantially different to that of adenovirus (Bellou et al., 2015; Schijven et al., 2003). Therefore, results based on bacteriophages may not always be representative to true pathogenic enteric viruses.

2.5. Numerical model approach and model setup

The axisymmetric modeling domain is shown in Fig. 1. The initial conditions were defined as a constant hydraulic head and zero virus concentration everywhere in the domain. The boundary conditions for the flow and virus transport equations are listed in Table 2. At boundary BC_1, the screen of the ASR well is situated where there is a constant flux of water into (during the injection phase) and out (during the recovery phase) of the domain. The value of dispersivity for nodes located in the well was set to zero allowing to implement Dirichlet boundary conditions ($C^*=1$) for virus injection at BC_1 during the injection phase. During the recovery phase, a zero dispersive flux was assigned for viruses at BC_1. At the boundary BC_2, it was assumed that the hydraulic

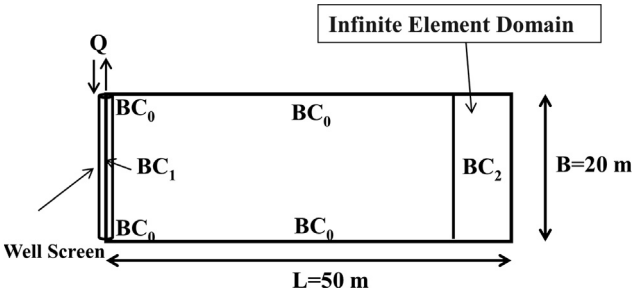

Fig. 1. Cross-section of the axisymmetrical modeling domain and boundary conditions BC_0 (no flux of water or virus), BC_1 (water and virus enter and leave the domain), and BC_2 (a constant head for water and zero virus concentration). Corresponding boundary condition equations for water flow and virus transport are listed in Table 2.

Table 2
Boundary conditions (see Fig. 1 for a schematic of the modeling domain).

Boundary	Description	Water flow	Virus transport
BC_0	No flux of water and virus across boundary	$\frac{\partial h}{\partial r}$ or $\frac{\partial h}{\partial z} = 0$	$\frac{\partial C^*}{\partial r}$ or $\frac{\partial C^*}{\partial z} = 0$
BC_1	Screen of the ASR well with a constant flux of water into (−) and out (+) of the domain	$\frac{\partial h}{\partial r} = \mp\frac{Q}{A_w k_r}$	$C^* = 1$ (during injection) $\frac{\partial C^*}{\partial r} = 0$ (during recovery)
BC_2	Right outer boundary, a constant head for water and zero virus concentration	$h = B$	$C^* = 0$

head is constant (equal to the aquifer thickness B in these simulations), and the virus concentration was zero. BC_0 designates no flux of water and viruses across the boundaries. The coupled groundwater flow and virus transport equations accounting for all the processes of attachment, detachment, inactivation, as well as physical and geochemical heterogeneities, were implemented and solved using COMSOL Multiphysics software (COMSOL, Inc., Palo Alto, CA 94301). We made use of the Infinite Element Domain feature of COMSOL. This feature performs a coordinate scaling in the radial direction to the selected domain such that boundary conditions on the outside of the infinite layer are effectively applied at a very large distance. Therefore, unwanted effects of artificial boundary conditions on the region of interest are suppressed. This allows modeling details in a transport domain, which is actually very large or infinite. The simulations were performed using a finite element mesh comprising 76,822 triangular elements. The optimal mesh resolution was determined by starting from a smaller number of elements and doubling the number until the concentration profiles from two consecutive meshes were found to be within a few percent (1–3%).

2.6. Numerical experiments

2.6.1. Virus transport in heterogeneous aquifer

Numerical experiments were initially conducted to highlight the capabilities of the model and provide some insight on the processes of virus transport during ASR in aquifers with different types of heterogeneity. In these simulations, aquifer heterogeneity was considered either as layered or random distributions of hydraulic conductivity with various standard deviations and correlation lengths. The basic values of the model parameters and their range of variation for the numerical simulations are listed in Table 1. The range of parameter values covered possible scenarios for virus transport in sandy aquifers, which has been determined in many field or laboratory studies (Schijven and Hassanizadeh, 2000).

2.6.2. Virus concentration in the recovered water

Additional simulations were conducted to examine the effect of removal parameters (attachment, detachment, and solid and aqueous phase inactivation), physical and chemical aquifer heterogeneity, and storage time on the extent of virus removal during ASR. In this case, normalized virus concentrations (C^*) in the recovered water at the ASR well were calculated for a range of aquifer heterogeneities (σ for ln(K), radial correlation length, and correlations of α with K), sticking efficiencies, detachment rates, solid phase inactivation rates, and storage durations that would be expected in the field. Note that the values of C^* were flux-averaged concentrations during the recovery phase. They were obtained after an injection phase of 60 days and plotted on a logarithmic scale as a function of recovery time. A constant mean K value of 5 m day^{-1} was assumed in all subsequent simulations. Moreover, all simulations were performed for a log-normally distributed K field with a given parameter set of σ, X, and Z. Unless otherwise mentioned the storage phase was neglected, and the recovery phase started immediately after the completion of 60 days of injection.

3. Results and discussion

3.1. Virus transport in an aquifer with distinct layered heterogeneity

Simulations in this section considered three distinct formation layers with different hydraulic conductivities. The value of K equaled 50, 5, and 25 m day^{-1} in the top, middle, and bottom layers, respectively. Fig. 2 presents distribution of normalized virus concentrations in the model domain after 30 days of injection. A constant value of $\alpha = 0$ (completely unfavorable for attachment) and $\alpha = 1 \times 10^{-4}$ was used in the top and bottom figures, respectively. The K value of the top layer was an order of magnitude larger than the K value in the layer below. Therefore, water in the top layer flowed faster than the other layers, and therefore most of the viruses migrated with the water flow through this more permeable layer. This example points out the paramount importance of preferential flow paths on virus transport. It is also noted that increasing α from 0 to 1×10^{-4} considerably lowered virus movement in the aquifer.

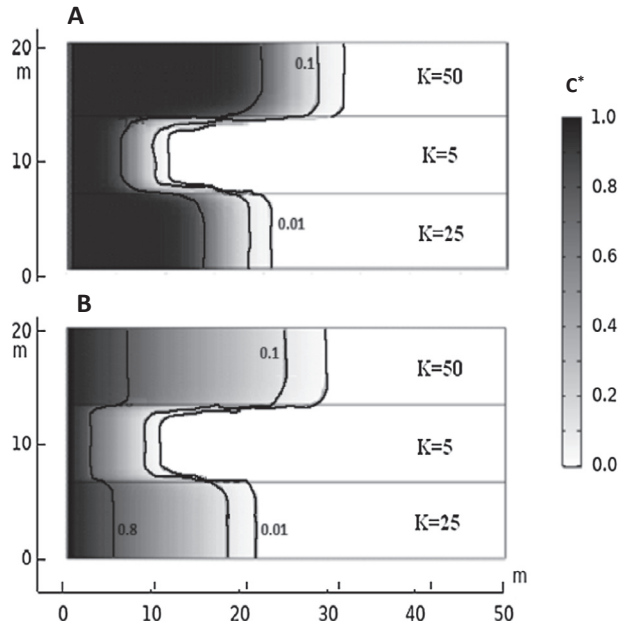

Fig. 2. Virus concentration profiles during the injection phase at $t = 30$ days for different layered hydraulic conductivity field as shown; (A) a uniform field of $\alpha = 0$ (zero attachment); (B) a uniform field of $\alpha = 1 \times 10^{-4}$. The values of other parameters are shown in Table 1. The contour labels indicate the normalized virus concentration C^*.

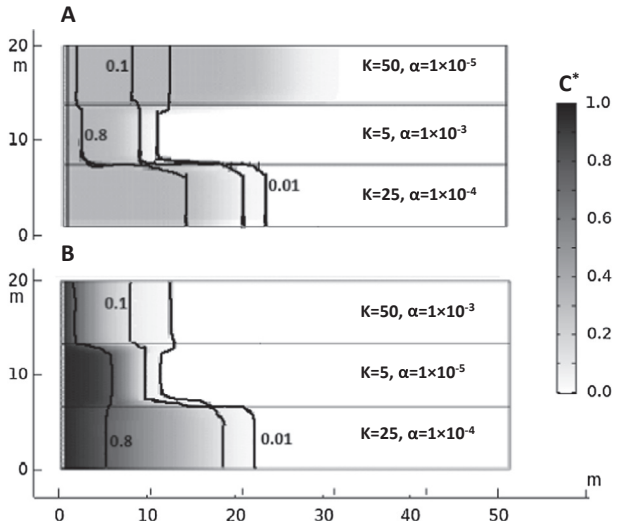

Fig. 3. Relative importance of combined effects of layered physical and geochemical heterogeneity on the transport of viruses in a model aquifer. The normalized virus concentration profiles are shown at $t = 30$ days for an aquifer containing three layers with different properties. The values of K and α for each layer are shown in each figure. The values of other parameters used in the simulations are listed in Table 1. The contour labels indicate the normalized virus concentration C^*.

Fig. 3 shows the combined effects of layered geochemical and physical heterogeneity on distribution of normalized virus concentrations in the aquifer after 30 days. The aquifer shown here consisted of three layers with the same value of K as in Fig. 2, but with different combinations of α. In Fig. 3A, an inverse relationship between K and α was assumed; e.g., values of α were assigned to be 1×10^{-5}, 1×10^{-3}, and 1×10^{-4} in the top, middle, and bottom layers, respectively. Conversely, a positive correlation between K and α was considered in Fig. 3B by assigning $\alpha = 1 \times 10^{-3}$, 1×10^{-5}, and 1×10^{-4} in the top, central, and bottom layer, respectively. All other conditions were kept the same in the two simulations. The results clearly show that a decreased attachment of viruses in the layer with the lowest value of α (1×10^{-5}) and highest value of K resulted in preferential migration of viruses through that layer (Fig. 3A). We observe that the combination of physical and geochemical heterogeneity significantly affected the movement patterns of viruses in the aquifer and that an inverse relationship between K and α was a worst-case (maximum) scenario for virus transport.

3.2. Virus transport in an aquifer with randomly distributed heterogeneity

The above simulations considered highly idealized scenarios, whereas natural aquifers can be highly heterogeneous with a log-normal distribution of K. In Fig. 4, we show the influence of a log-normal distributed K (with a mean value of 5 m day^{-1}) on virus transport in the aquifer. The simulations were performed for a $\bar{\alpha}$ value of 1×10^{-4} and the localized value of α was correlated to the value of K through Eq. [6] with $\omega = -0.1$. Under such conditions, variations of K led to local variations of the pore water velocity, d_{50}, and α in the aquifer. Therefore, spatial variability of these parameters resulted in local variations of K_{att} (Eqs. [4–6]). Fig. 4 shows the simulated distribution of normalized virus concentrations in the aquifer after 30 days of injection. In this case, the value of σ for ln(K) (e.g., the physical heterogeneity) increased from 0.7, 1.4, and 2.1 in the top, middle, and bottom figures, respectively. The correlation lengths of X and Z were taken as 0.5 in these simulations. The virus concentration variability and location of the front tended to increase with an increase in σ. Maximum and minimum values of K in the model domain increased and decreased, respectively, with increasing σ. For example, values of K

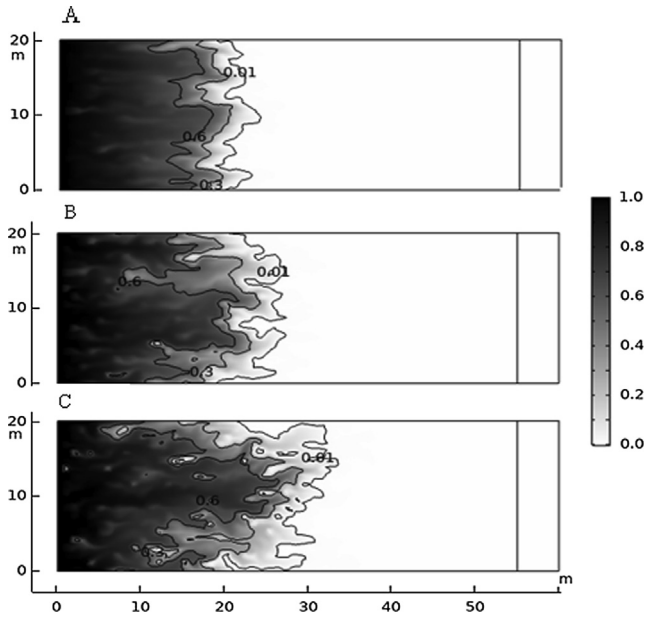

Fig. 4. Influence of randomly distributed hydraulic conductivity on virus transport. The simulations were performed for a continuous injection of viruses at the ASR well for 30 days. The value of α was set to 1×10^{-4} and α was correlated with K through Eq. (6). The three plots represent the virus concentration distribution (C^*) after 30 days. In all cases, the K field was generated using a mean value of $K = 5\,\mathrm{m\,day^{-1}}$ and correlation lengths of 0.5. The standard deviations (σ) of ln(K) were (A) 0.7, (B) 1.4, and (C) 2.1. The values of other parameters used in the simulations are shown in Table 1.

exhibited two orders of magnitude variations for $\sigma = 2.1$. Locations with high K provided preferential pathways for virus transport, whereas low K regions behaved as natural barriers to flow that decreased the transport of viruses. Virus concentrations were therefore very low in regions with low K (see lighter shades in Fig. 4C).

Fig. 5 presents the virus concentration distribution when σ of ln(K) was 2.1, the vertical correlation length (Z) was 0.5 m, and the radial correlation length (X) was 5 m (Fig. 5A) and 50 m (Fig. 5B). The results illustrate that the virus concentration fronts moved faster in regions with higher value of X. When the value of $X = 50$ m, zones with higher

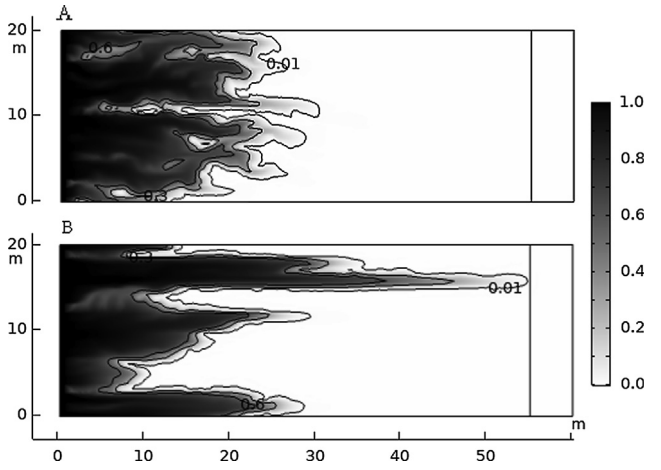

Fig. 5. Influence of randomly distributed hydraulic conductivity on virus transport. The value of $\bar{\alpha}$ was set to 1×10^{-4} and α was correlated with K using Eq. (6). The two plots represent the virus concentration distribution (C^*) after 30 days of injection. In all cases, the K field was generated using a mean value of $K = 5\,\mathrm{m\,day^{-1}}$. The standard deviation (σ) of ln(K) was 2.1 with (A) $X = 5$ m and $Z = 0.5$ m and (B) $X = 50$ m and $Z = 0.5$ m. The values of other parameters used in the simulations are listed in Table 1.

hydraulic conductivity, acting as preferential pathways, were more connected in which the virus advection velocity was significantly higher. In addition, the rate of virus attachment through the high K zones decreases with increasing flow velocity, resulting in less attenuated virus concentration profile. The low velocity regions with depleted virus transport are also more prevalent for larger value of X. Consequently, greater non-uniformity of the virus concentration front occurred for larger radial correlation length which yielded greater deviations from the homogeneous aquifer with uniform fronts. The effect of heterogeneity was also evident in the distribution of conservative tracer concentrations which showed more dispersion than the homogeneous case (data not shown).

3.3. Virus concentration in the recovered water

3.3.1. Sensitivity to aquifer heterogeneity

To explore the impact of spatial variability of K on virus concentration in the recovered water, a series of simulations was performed with different values of σ of ln(K). Values of $\sigma = 0.7$, 1.44, and 2.1 were chosen to represent low, intermediate, and high levels of heterogeneity in K, respectively. In these simulations, detachment and inactivation coefficients were set to zero and thus virus removal occurred only due to irreversible virus attachment to aquifer sediments. In addition, the value of $\bar{\alpha}$ was set to 1×10^{-3}, which was a relatively conservative value based on many laboratory and field studies (Sasidharan et al., 2018; Sasidharan et al., 2017). Note that the localized values of α and d_{50} were correlated to the value of K through equations (5) and (6). A similar simulation was also performed for the homogeneous aquifer ($\sigma = 0$) with a hydraulic conductivity of $5\,\mathrm{m\,day^{-1}}$ for comparison purposes.

Fig. 6 shows values of C^* as a function of recovery time for aquifers with various degrees of heterogeneity. Note that at the start of the recovery phase, the virus concentration was the same as the input concentration during the injection phase (i.e. $C^* = 1$) because the inactivation of viruses was not considered. As expected, virus concentration in the recovered water decreased over the recovery time. For example, a more than 2 $\log_{10}$ reduction in virus concentration

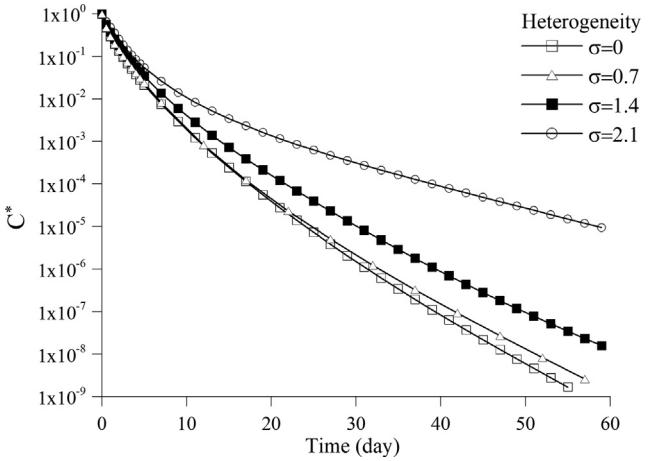

Fig. 6. Normalized virus concentrations at the ASR well as a function of recovery time obtained from heterogeneous and homogeneous simulations following 60 days of injection. Values of σ of ln(K) were 0.7, 1.44, and 2.1 to represent low, intermediate, and high levels of heterogeneity in K field with mean K of $5\,\mathrm{m\,day^{-1}}$. Detachment and inactivation coefficients were set to zero and thus virus removal occurred only due to virus attachment to aquifer sediments. The value of $\bar{\alpha}$ was set to 1×10^{-3} and the localized values of α and d_{50} were correlated to K according to equations (5) and (6). A similar simulation was also performed for the homogeneous aquifer ($\sigma = 0$) with a hydraulic conductivity of $5\,\mathrm{m\,day^{-1}}$ for comparison purposes. The values of other parameters used in the simulations are shown in Table 1.

occurred after approximately 10 days of water recovery. Differences in C^* for the heterogeneous and homogeneous aquifers were initially small because the recovered viruses had only traveled short distances in the aquifer and experienced little attachment. However, differences in C^* for the heterogeneous and homogeneous aquifers increased at later stages of recovery, especially for higher values of σ. For example, the values of C^* for the heterogeneous aquifer with $\sigma = 2.1$ was around 4 orders of magnitude higher than those for the homogeneous aquifer by the end of the recovery phase (day 60). This reflects a decrease in virus removal with an increase in aquifer physical heterogeneity. For example, a 3 $\log_{10}$ (0.001) reduction in the virus concentration occurred after 21, 13, 8, and 7 days when σ of ln(K) equaled 2.1, 1.4, 0.7, and 0, respectively.

The difference between virus removal for heterogeneous and homogeneous cases can be attributed to spatially variable v, α, and d_{50} which also results in heterogeneity in K_{att}. In higher permeable zones a decrease in virus attachment occurs due to lower K_{att}. Conversely, an increased virus removal is expected in lower permeable zones due to higher K_{att}. The slight difference between the results from homogeneous and heterogeneous aquifers with $\sigma = 0.7$ is attributed to the fact that the volume of high permeability zones was small and they were mainly isolated. Therefore, viruses were likely to encounter low permeable zones during their transport in the aquifer which produced higher virus attachment. Consequently, spatial variability of K in an aquifer with low amounts of heterogeneity may not have a large influence on virus removal during ASR. Conversely, more volume of the aquifer was characterized by the tails of the K distribution when σ increased to 1.4 or 2.1. The "high K" tail may be thought of as highly conductive regions with small values K_{att}. Note that the relationship between K_{att} and K was highly nonlinear, and resulted in significant decreases in K_{att} with increasing K. Therefore, when the volume of highly conductive zones was increased with increasing σ, these zones acted as preferential pathways for virus transport with less chance of encountering low permeability zones. The model simulations suggest that reduced virus removal is expected in aquifers with high σ compared to homogeneous aquifers.

An additional suite of simulations was conducted to explore the impact of the radial correlation length (X) on virus removal during the ASR operation. Three different values for the radial correlation length ($X = 0.5$, 5, and 50) were examined for a fixed value of $\sigma = 1.4$. Recall that the radial correlation length is a measure of the radial distance that similar values of K are maintained. Fig. 7 shows the values of C^* in the recovered water when $X = 0.5$, 5, and 50 m. Less virus removal occurred as the value of X was increased. For example, the virus concentration after 30 days of recovery only decreased by 2.5 $\log_{10}$ when $X = 50$ m, whereas it was reduced by 5 $\log_{10}$ when $X = 0.5$ (Fig. 7). These results indicate that virus removal might be significantly lower in aquifers when high permeability zones with low virus attachment rates (higher d_{50} and lower α) are laterally connected to greater lengths (higher X). In contrast, an aquifer with a smaller value of X, comprising many isolated high permeability zones, provides significantly higher levels of virus removal. The significant difference between the homogeneous and heterogeneous aquifers when σ and X were high, highlights the importance of physicochemical heterogeneity on the virus removal performance during ASR.

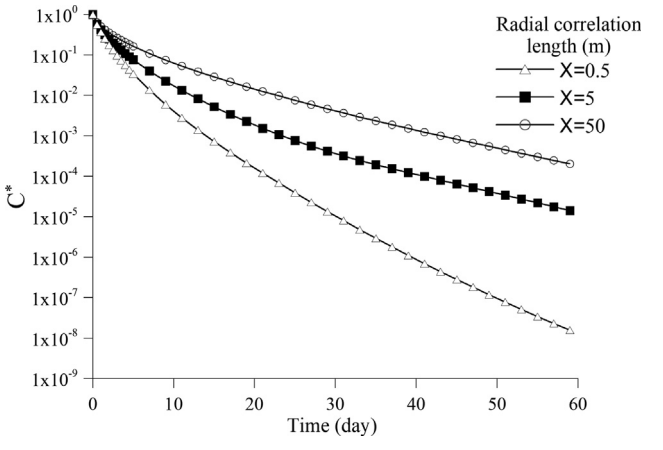

Fig. 7. Normalized virus concentrations at the ASR well as a function of recovery time obtained from a heterogeneous aquifer when σ of ln(K) was 1.44 and the correlation length in radial direction (X) was 0.5, 5, and 50 m. Results obtained after 60 days of injection and for the mean K value of 5 m day^{-1}. Detachment and inactivation coefficients were set to zero and the value of $\bar{\alpha}$ was set to 1×10^{-3}. The values of other parameters used in the simulations are shown in Table 1.

3.3.2. Influence of sticking efficiency

For the previous simulations, we assumed that the mean sticking efficiency ($\bar{\alpha}$) was 1×10^{-3}. However, this model parameter can vary by orders of magnitude (Hornstra et al., 2018; Bradford and Torkzaban, 2013; Bradford and Torkzaban, 2015; Chu et al., 2003). The sticking efficiency is a function of the water chemistry as well as virus and sediment surface properties (Knappett et al., 2008; Pham et al., 2009; Sadeghi et al., 2013). An additional series of simulations was therefore carried out to explore the impact of the sticking efficiency on virus removal during ASR in heterogeneous aquifers. In these simulations, the value of $\bar{\alpha}$ varied across the heterogeneous aquifer because it was correlated with K using Eq. [6], and the values of detachment and inactivation rate coefficients were set to zero. Fig. 8 presents plots of the predicted influence of $\bar{\alpha}$ on recovered C^* in an aquifer with $\sigma = 1.4$ and a horizontal correlation length of 50 m. This value of $\sigma = 1.4$ was chosen to represent an intermediate level of heterogeneity in K. Other model parameters are given in Table 1. It is noted that increasing $\bar{\alpha}$ from 1×10^{-5} to 1×10^{-2} significantly increased the removal of viruses. For example, when $\bar{\alpha}$ was 1×10^{-2}, the values of C^* were found to reduce by almost 5 $\log_{10}$ in less than 5 days of water recovery. Conversely, decreasing $\bar{\alpha}$ to 1×10^{-5} resulted in little virus removal; e.g., C^* was reduced by less than 0.5 $\log_{10}$ after 60 days. In this case, the behavior of virus transport in the aquifer was somewhat similar to that of a conservative tracer. These simulation results indicate that characterization of $\bar{\alpha}$ for a given aquifer appears to be an important consideration for accurately quantifying field-scale virus removal during the ASR operation.

3.3.3. Influence of virus detachment

Consistent with the colloid filtration theory (Eq. (4)) the previous simulations assumed irreversible virus attachment onto the sediment

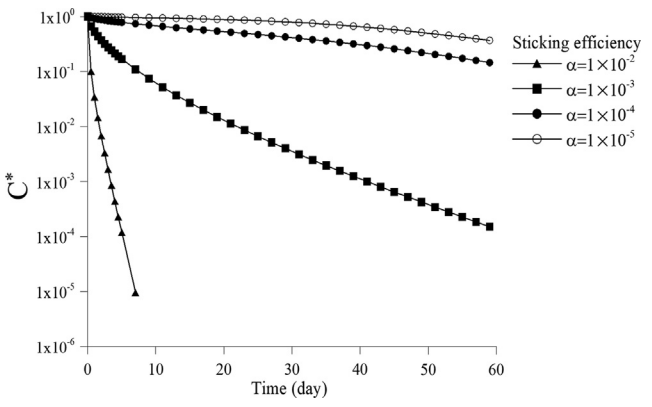

Fig. 8. Influence of sticking efficiency (α) on virus removal during ASR in a heterogeneous aquifer. Normalized virus concentrations were obtained at the ASR well during the recovery phase after 60 days of injection. The standard deviation (σ) of ln(K) was 1.4 with $X = 50$ m and $Z = 0.5$ m. The localized value of α was correlated with K using Eq. (6). The values of other parameters used in the simulations are shown in Table 1.

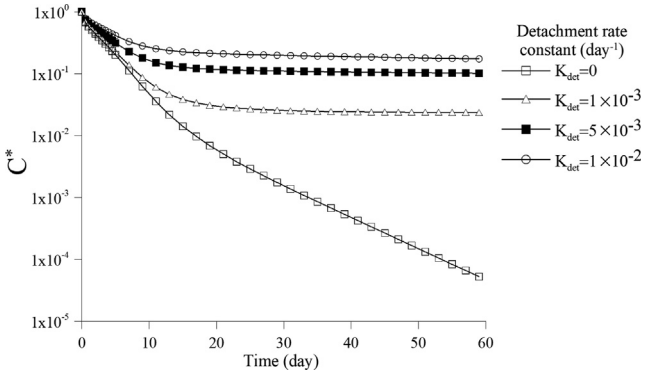

Fig. 9. Influence of virus detachment rate constants (K_{det}) on virus removal during ASR in a heterogeneous aquifer. Normalized virus concentrations were obtained at the ASR well during the recovery phase after 60 days of injection. The standard deviation (σ) of ln(K) was 1.4 with $X = 5$ m and $Z = 0.5$ m. The value of $\bar{\alpha}$ was set to 1×10^{-3} and the localized α was correlated with K using Eq. [6]. The values of other parameters used in the simulations are shown in Table 1.

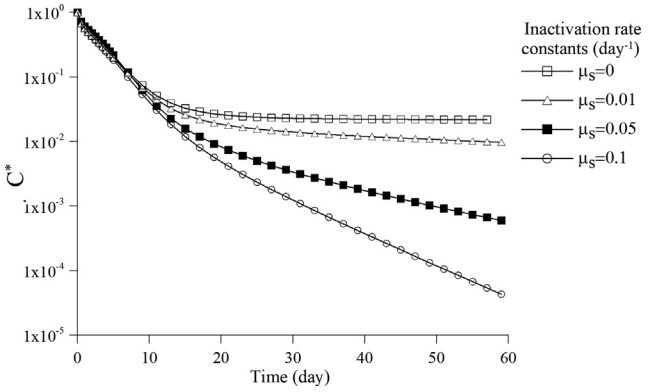

Fig. 10. Influence of inactivation rate constants (μ_s) of attached viruses on virus removal during ASR in a heterogeneous aquifer. Normalized virus concentrations were obtained at the ASR well during the recovery phase after 60 days of injection. The transport parameters were taken as follows: $\sigma = 2.1$; $X = 5$ m; $Z = 0.5$ m; $\bar{\alpha} = 0.001$; $K_{det} = 0.001$ day^{-1}; $\mu_l = 0.01$ day^{-1}. The values of other parameters used in the simulations are shown in Table 1.

surfaces. This assumption has been confirmed in studies involving oppositely charged viruses and collector surfaces (Foppen et al., 2006; Torkzaban et al., 2006). On the other hand, transport studies involving similarly charged viruses and collector surfaces have shown a finite rate of virus detachment (Sasidharan et al., 2017; Schijven et al., 2003). Hence, a series of simulations were performed to assess the importance of virus detachment on the removal of viruses in a heterogeneous aquifer with $\sigma = 1.44$ and $X = 5$ m. Fig. 9 presents illustrative examples of the predicted influence of K_{det} (0, 0.001, 0.005, 0.01 day^{-1}) on C^* in the recovered water. In these simulations, the value of $\bar{\alpha}$ was set to 1×10^{-3} and no virus inactivation was considered. Increasing the value of K_{det} from zero to 0.01 day^{-1} increased the concentration of viruses in the recovered water, especially at later stages of recovery. For example, the concentration of viruses after 30 days of recovery was reduced by 3 $\log_{10}$ when the K_{det} was zero compared to less than 1 $\log_{10}$ reduction when K_{det} was 0.01 day^{-1}. It should be mentioned that the magnitude of detachment rate constants of viruses from natural surfaces can vary widely and depends on the relative strengths of the adhesive and the diffusive forces (Schijven and Hassanizadeh, 2000; Torkzaban et al., 2015). However, the rate coefficient for virus attachment has typically been reported to be higher than that for virus detachment in field (Bales et al., 1997; Schijven et al., 1999) and laboratory (Sasidharan et al., 2018; Shen et al., 2012) studies.

3.3.4. Influence of solid phase inactivation and storage time

To explore the impact of solid phase inactivation (μ_s) on virus removal during ASR, a series of simulations was conducted with different values of μ_s. Fig. 10 shows values of C^* during the recovery phase from a heterogeneous aquifer when μ_s ranged from 0 to 0.1 day^{-1}. The other transport parameters were taken as follows: $\sigma = 2.1$; $X = 5$ m; $Z = 0.5$ m; $\bar{\alpha} = 0.001$; $K_{det} = 0.001$ day^{-1}; and $\mu_l = 0.01$ day^{-1}. Note that a heterogeneous domain with a very large σ provides a worst-case scenario for determining virus transport and risk assessment. As expected, increasing μ_s produced greater amounts of virus reduction in the recovered water due to enhanced inactivation of attached viruses on the sediment surfaces. In the initial periods of recovery phase, the effect of μ_s on enhancing virus removal was small because of the short residence time for virus attachment and inactivation. Conversely, μ_s had a marked effect on reducing C^* in later stages of recovery. Virus transport models which does not incorporate the effect of solid phase inactivation of attached viruses may, therefore, result in erroneous results for the extent of virus removal in ASR schemes.

Inactivation occurs when viruses lose their ability to infect host cells and replicate because of disruption of proteins and/or the degradation of nucleic acid (Gerba, 1983). The most important factors affecting the virus inactivation rate include temperature, groundwater microbial activity, pH, salt species and concentration, and virus type (McCarthy and McKay, 2004; Schijven and Hassanizadeh, 2000). The inactivation rate coefficient for human enteric viruses in groundwater, determined at several MAR sites in Australia, was found to be very small (~0.01 day^{-1}) (Sidhu et al., 2015). However, attachment of viruses to mineral surfaces appears to play an important role in virus inactivation. Many researchers have reported that virus inactivation is generally accelerated when they are attached to solid surfaces compared to those in the liquid phase (Ryan et al., 2002; Sasidharan et al., 2018; Schijven et al., 1999). This enhanced inactivation has been attributed to strong adhesive forces between viruses and mineral surfaces (Harvey and Ryan, 2004). In addition, some research has indicated that the strength of virus attachment may also increase with the residence time (Mondon et al., 2003; Torkzaban et al., 2013; Vadillo-Rodriguez et al., 2004; Xu and Logan, 2006), and this may further enhance solid phase inactivation.

3.3.5. Effects of storage phase

Up to this point, the storage phase of the ASR operation has been neglected to focus the discussion on virus removal processes in heterogeneous aquifers during the injection and recovery phases. However, the storage phase is an important component of an ASR scheme during which viruses are transported in the aquifer with the native groundwater flow. In this section, the effect of the duration of storage phase on virus removal is investigated. The groundwater velocity during the storage phase was determined based on a regional hydraulic gradient of 0.001. We also assumed that K_{att} during the storage phase was described with Eq. (4). In these simulations, the value of μ_s was set to 0.05 day^{-1} and values of other parameters were the same as those for the simulations shown in Fig. 10. For the conditions investigated in Fig. 11, increasing the duration of storage phase resulted in a greater amount of virus removal. The marked effect of storage phase on the extent of virus removal is attributed to the higher value of μ_s employed in these simulations. As expected, larger values of μ_s result in a greater decrease of the concentration of infective attached viruses during the storage phase. Therefore, the rate of virus detachment is decreased and less viruses can be detected in the recovered water.

3.4. Virus removal for an ASR case study

An additional suite of simulations was conducted to evaluate virus removal in an ASR scheme by assuming the transport parameters as

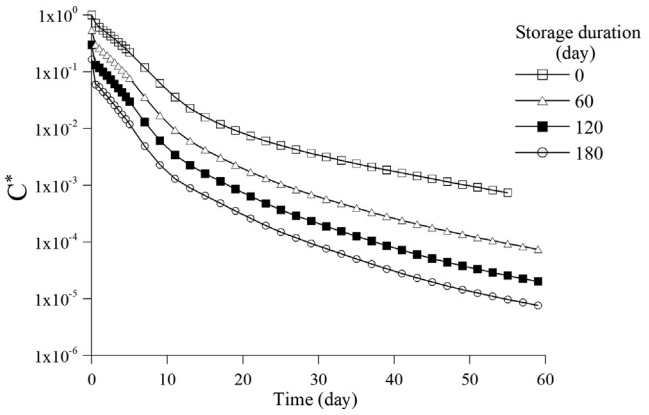

Fig. 11. Normalized virus concentrations at the ASR well as a function of recovery time obtained from a heterogeneous aquifer for four different durations of storage phase. Results obtained after 60 days of injection and the mean K value of 5 m day^{-1}. The model parameters were taken as follows: $\sigma = 2.1$; $X = 5$ m; $Z = 0.5$ m; $\bar{\alpha} = 0.001$; $K_{det} = 0.001$ day^{-1}; $\mu_l = 0.01$ day^{-1}, $\mu_s = 0.05$ day^{-1}. The groundwater velocity was determined based on a regional hydraulic gradient of 0.001. The values of other parameters used in the simulations are shown in Table 1.

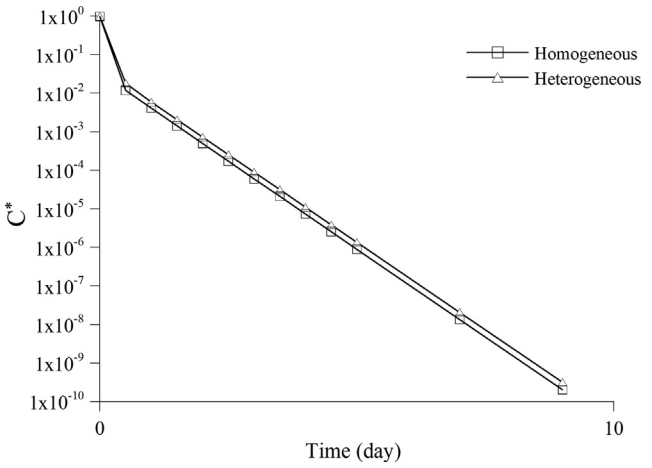

Fig. 12. Normalized virus concentrations at the ASR well as a function of recovery time obtained from a heterogeneous and homogeneous aquifer. Results obtained after 60 days of injection and the mean K value was 5 m day^{-1}. The model parameters were taken as follows: $\bar{\alpha} = 0.145$; $K_{det} = 0.23$ day^{-1}; $\mu_s = 2.0$ day^{-1}; $\mu_l = 0.07$ day^{-1}. These values are reported in Sasidharan et al. (2017) for three different bacteriophages obtained from column experiments packed with sediment and stormwater collected from a MAR site in Parafield, Australia. The stochastic parameters for the heterogeneous aquifer were taken as $\sigma = 2.07$; $X = 50$ m in order to represent a highly heterogeneous aquifer. Moreover, the storage phase was ignored, and water recovery started immediately after 60 days of injection. The values of other parameters used in the simulations are shown in Table 1.

follows: $\bar{\alpha} = 0.145$; $K_{det} = 0.23$ day^{-1}; $\mu_s = 2.0$ day^{-1}; $\mu_l = 0.07$ day^{-1}. These are averaged values obtained for three different bacteriophages (MS2, PRD1, and ΦX174) for a limestone aquifer reported in (Sasidharan et al. (2017). In that study, the transport of bacteriophages was studied in column experiments packed with sediment and stormwater collected from an ASR site in Parafield, SA, Australia. Virus breakthrough concentrations (BTCs) were successfully simulated using an advective–dispersive model that accounted for rates of attachment (K_{att}), detachment (K_{det}), and solid phase inactivation (μ_s). We employed the reported fitted values of K_{det}, μ_s, measured μ_l, and calculated $\bar{\alpha}$ in our model to evaluate the removal of viruses in both homogeneous and heterogeneous aquifers. The stochastic parameters for the heterogeneous aquifer were taken as $\sigma = 2.07$, $Z = 5$ m, and $X = 50$ m to represent a highly heterogeneous aquifer with K values exhibiting three orders of magnitude variations and many connected high permeable lenses in the radial direction. Other model parameters are given in Table 1. Moreover, the storage phase was ignored, and the recovery phase was immediately started after 60 days of injection.

The combined effects of $\bar{\alpha}$, K_{det}, μ_s, and μ_l yielded interesting results (Fig. 12). Under the examined conditions, model results demonstrate that virus removal was significantly higher than those obtained in our previous simulations because of greater rate constants of virus attachment and inactivation reported for the aquifer sediment. Consequently, the vast majority of viruses were attached and subsequently inactivated on the solid phase within just a few meters from the ASR well. For example, virus concentration decreased by 6 $\log_{10}$ after about 5 days of recovery. This time corresponds to a travel distance of 7.6 m from the well. The results show that differences between the magnitudes of virus removal for heterogeneous and homogeneous cases were negligible. Because values of α and μ_s reported for this case study were significantly high, the spatial distribution of water velocities only had a slight influence on the recovered concentrations of viruses. These findings imply that if stormwater needs a 6 $\log_{10}$ (1 million-fold) reduction in virus concentration before it can serve as drinking water, the practice of ASR will lead to 92% of the recovered water will meet the requirement. The remaining 8% of the initial recovered water that exceeds this threshold should be further treated or discarded.

4. Concluding remarks

The results of this study demonstrate that incorporation of aquifer heterogeneity has a marked effect on the prediction of virus transport and removal during ASR. Both layered and log-normally distributed heterogeneity can result in substantial changes in virus transport patterns. Our modeling results indicate that incorporation of aquifer heterogeneity resulted in faster virus transport and smaller virus removal during ASR compared to those of a homogeneous aquifer. In order to predict the virus treatment capacity of the aquifer in an ASR scheme, some information regarding the degree of aquifer heterogeneity would, therefore, be required.

The model also provides a valuable insight on the impact of various removal processes such as attachment, detachment, and solid phase virus inactivation. The virus sticking efficiency and surface inactivation terms were found to have a great influence on virus concentrations during the recovery phase. Large detachment constants may result in an increased virus concentration in the recovered water during the recovery phase unless the surface inactivation rate is very large. Furthermore, the model simulations showed that the solid phase inactivation had a greater influence on the overall virus removal compared to the liquid phase inactivation under realistic field conditions.

Results of this study suggest that simpler models that account for virus transport through a homogeneous aquifer and ignore the influence of aquifer heterogeneity and surface inactivation may yield a misleading picture of virus removal during ASR. It is important to accurately quantify the virus sticking efficiency, detachment, and inactivation of viruses by at least conducting a series of laboratory column experiments employing aquifer sediments. One way to potentially minimize the risk of viruses during ASR operations is to provide an adequate residence time for solid phase inactivation. This model, coupled with reliable estimates of virus removal parameters, may lead to adequate predictions of natural treatment performance of aquifers targeted for ASR schemes.

Quantitative microbial risk assessment calculations for MAR systems have considered that liquid phase virus inactivation was the only reliable mechanism for virus removal in the aquifer, and neglected processes of virus attachment, detachment, and solid phase inactivation (Dillon et al., 2008; Page et al., 2016). Results from this study provide valuable insight on the relative importance of these removal processes

for viruses during ASR and indicate that microbial risk assessments that only consider liquid phase inactivation may be overly conservative in many instances. Recognizing the removal of viruses via irreversible attachment and/or solid phase inactivation during aquifer storage would help to eliminate some of the expensive post-treatment for recovered MAR water. Stormwater harvesting coupled to ASR provides a great opportunity to reuse this valuable resource that is often wasted. Aquifers can act as a treatment barrier within a multiple-barrier approach to harvest and reuse urban stormwater.

Declaration of Competing Interest

The authors declare that they have no known competing financial interests or personal relationships that could have appeared to influence the work reported in this paper.

References

Anders, R., Chrysikopoulos, C.V., 2005. Virus fate and transport during artificial recharge with recycled water. Water Resour. Res. 41 (10), W10415.

Anders, R., Chrysikopoulos, C.V., 2006. Evaluation of the factors controlling the time-dependent inactivation rate coefficients of bacteriophage MS2 and PRD1. Environ. Sci. Technol. 40 (10), 3237–3242.

Bales, R.C., Li, S., Yeh, T.-C.J., Lenczewski, M.E., Gerba, C.P., 1997. Bacteriophage and microsphere transport in saturated porous media: forced-gradient experiment at Borden, Ontario. Water Resour. Res. 33 (4), 639–648.

Bear, J., 1972. Dynamics of Fluids in Porous Materials. Society of Petroleum Engineers, Dallas, TX, USA.

Bellou, M.I., Syngouna, V.I., Tselepi, M.A., Kokkinos, P., Paparrodopoulos, S.C., Vantarakis, A., Chrysikopoulos, C.V., 2015. Interaction of human adenoviruses and coliphages with kaolinite and bentonite. Sci. Total Environ. 517, 86–95.

Bhattacharjee, S., Ryan, J.N., Elimelech, M., 2002. Virus transport in physically and geochemically heterogeneous subsurface porous media. J. Contaminant Hydrol. 57 (3–4), 161–187. https://doi.org/10.1016/S0169-7722(02)00007-4.

Bradford, S.A., Torkzaban, S., 2013. Colloid interaction energies for physically and chemically heterogeneous porous media. Langmuir 29 (11), 3668–3676. https://doi.org/10.1021/la400229f.

Bradford, S.A., Torkzaban, S., 2015. Determining parameters and mechanisms of colloid retention and release in porous media. Langmuir 31 (44), 12096–12105. https://doi.org/10.1021/acs.langmuir.5b03080.

Bradford, S.A., Leij, F.J., Schijven, J., Torkzaban, S., 2017. Critical role of preferential flow in field-scale pathogen transport and retention. Vadose Zone J. 16. https://doi.org/10.2136/vzj2016.12.0127.

Chrysikopoulos, C.V., Aravantinou, A.F., 2012. Virus inactivation in the presence of quartz sand under static and dynamic batch conditions at different temperatures. J. Hazard. Mater. 233–234, 148–157. https://doi.org/10.1016/j.jhazmat.2012.07.002.

Chrysikopoulos, C.V., Sim, Y., 1996. One-dimensional virus transport homogeneous porous media with time dependent distribution coefficient. J. Hydrol. 185, 199–219. https://doi.org/10.1016/0022-1694(95)02990-7.

Chu, Y., Jin, Y., Baumann, T., Yates, M.V., 2003. Effect of soil properties on saturated and unsaturated virus transport through columns. J. Environ. Quality 32 (6), 2017–2025.

Dagan, G., Fiori, A., Jankovic, I., 2003. Flow and transport in highly heterogeneous formations: 1. Conceptual framework and validity of first-order approximations. art No. 1268. Water. Resour. Res. 39 (9), 12. https://doi.org/10.1029/2002WR001717.

Dillon, P., et al., 2008. A critical evaluation of combined engineered and aquifer treatment systems in water recycling. Water Sci. Technol. 753–762. https://doi.org/10.2166/wst.2008.168.

Dillon, P., et al., 2010. Managed aquifer recharge: rediscovering nature as a leading edge technology. Water Sci. Technol. 62 (10), 2338–2345. https://doi.org/10.2166/wst.2010.444.

Foppen, J.W., Okletey, S., Schijven, J.F., 2006. Effect of goethite coating and humic acid on the transport of bacteriophage PRD1 in columns of saturated sand. J. Contaminant Hydrol. 85 (3–4), 287–301. https://doi.org/10.1016/j.jconhyd.2006.02.004.

Freeze, R.A., 1975. A stochastic-conceptual analysis of one-dimensional groundwater flow in nonuniform homogeneous media. Water Resour. Res. 11 (5), 725–741.

Garabedian, S., Gelhar, L., Celia, M., 1988. Large-scale dispersivae transport in aquifers: Field experiments and reactive transport theory. Parsons Laboratory Report 315. MIT, Cambridge.

Gerba, C.P., 1983. Virus survival and transport in groundwater. Developments in Industrial Microbiology (USA).

Harvey, R.W., Kinner, N.E., MacDonald, D., Metge, D.W., Bunn, A., 1993. Role of physical heterogeneity in the interpretation of small-scale laboratory and field observations of bacteria, microbial-sized microsphere, and bromide transport through aquifer sediments. Water Resour. Res. 29 (8), 2713–2721.

Harvey, R.W., Ryan, J.N., 2004. Use of PRD1 bacteriophage in groundwater viral transport, inactivation, and attachment studies. FEMS Microbiol. Ecol. 49 (1), 3–16. https://doi.org/10.1016/j.femsec.2003.09.015.

Hornstra, L.M., Schijven, J.F., Waade, A., Prat, G.S., Smits, F.J.C., Cirkel, G., Stuyfzand, P.J., Medema, G.J., 2018. Transport of bacteriophage ms2 and prd1 in saturated dune sand under suboxic conditions. Water Res. 139, 158–167.

Hsu, B.B., Wong, S.Y., Hammond, P.T., Chen, J., Klibanov, A.M., 2011. Mechanism of inactivation of influenza viruses by immobilized hydrophobic polycations. Proc. Natl. Acad. Sci. U.S.A. 108 (1), 61–66.

Ibaraki, M., Sudicky, E., 1995. Colloid-facilitated contaminant transport in discretely fractured porous media: 1. Numerical formulation and sensitivity analysis. Water Resour. Res. 31 (12), 2945–2960.

Jarvis, N., Larsbo, M., 2012. MACRO (v5. 2): Model use, calibration, and validation. Transactions of the ASABE, 55(4): 1413–1423.

Jin, Y., Flury, M., 2002. Fate and transport of viruses in porous media. Adv. Agronomy 77, 39–102.

Katzourakis, V.E., Chrysikopoulos, C.V., 2018. Impact of spatially variable collision efficiency on the transport of biocolloids in geochemically heterogeneous porous media. Water Resour. Res. 54 (6), 3841–3862.

Kitanidis, P.K., 1997. Groundwater Flow in Heterogeneous Formations in Subsurface Flow and Transport: The Stochastic Approach, edited by G. Dagan, Ê S.P. Neuman, pp. 83–91, Cambridge Univ. Press, 1997.

Knappett, P.S., Emelko, M.B., Zhuang, J., McKay, L.D., 2008. Transport and retention of a bacteriophage and microspheres in saturated, angular porous media: effects of ionic strength and grain size. Water Res. 42 (16), 4368–4378. https://doi.org/10.1016/j.watres.2008.07.041.

Masciopinto, C., La Mantia, R., Chrysikopoulos, C.V., 2008. Fate and transport of pathogens in a fractured aquifer in the Salento area, Italy. Water Resour. Res. 44 (1), W01404. https://doi.org/10.1029/2006WR005643.

Maxwell, R.M., Welty, C., Harvey, R.W., 2007. Revisiting the Cape Cod bacteria injection experiment using a stochastic modeling approach. Environ. Sci. Technol. 41 (15), 5548–5558.

McCarthy, J.F., McKay, L.D., 2004. Colloid transport in the subsurface: past, present, and future challenges. Vadose Zone J. 3 (2), 326–337.

Mejia, J.M., Rodriguez-Iturbe, I., 1974. On the synthesis of random field sampling from the spectrum: an application to the generation of hydrologic spatial processes. Water Kesour. Hes. 10 (4), 705–711.

Messina, F., Marchisio, D.L., Sethi, R., 2015. An extended and total flux normalized correlation equation for predicting single-collector efficiency. J. Colloid Interface Sci. 446, 185–193. https://doi.org/10.1016/j.jcis.2015.01.024.

Mondon, M., Berger, S., Ziegler, C., 2003. Scanning-force techniques to monitor time-dependent changes in topography and adhesion force of proteins on surfaces. Anal. Bioanal. Chem. 375 (7), 849–855. https://doi.org/10.1007/s00216-003-1751-2.

Morley, L.M., Hornberger, G.M., Mills, A.L., Herman, J.S., 1998. Effects of transverse mixing on transport of bacteria through heterogeneous porous media. Water Resour. Res. 34 (8), 1901–1908.

NRMMC-EPHC-NHMRC, 2009. National Water Quality Management Strategy, Australian guidelines for water recycling: Managing health and environmental risks (phase 2) Managed Aquifer Recharge. In: Council, N.R.M.M., Council, E.P.a.H., Council, N.H.a.M.R. (Eds.), National Water Quality Management Strategy, Canberra.

Page, D., et al., 2016. Assessment of treatment options of recycling urban stormwater recycling via aquifers to produce drinking water quality. Urban Water J. 1–6. https://doi.org/10.1080/1573062X.2015.1024691.

Pang, L., 2009. Microbial removal rates in subsurface media estimated from published studies of field experiments and large intact soil cores. J. Environ. Qual. 38 (4), 1531–1559. https://doi.org/10.2134/jeq2008.0379.

Pham, M., Mintz, E.A., Nguyen, T.H., 2009. Deposition kinetics of bacteriophage MS2 to natural organic matter: role of divalent cations. J. Colloid Interface Sci. 338 (1), 1–9. https://doi.org/10.1016/J.Jcis. 2009.06.025.

Rehmann, L.L.C., Welty, C., Harvey, R.W., 1999. Stochastic analysis of virus transport in aquifers. Water Resour. Res. 35 (7), 1987–2006.

Reynolds, K.A., Mena, K.D., Gerba, C.P., 2008. Risk of waterborne illness via drinking water in the United States, Reviews of environmental contamination and toxicology. Springer, pp. 117–158.

Rockhold, M.L., Yarwood, R., Selker, J.S., 2004. Coupled microbial and transport processes in soils. Vadose Zone J. 3 (2), 368–383.

Ryan, J.N., et al., 2002. Field and laboratory investigations of inactivation of viruses (PRD1 and MS2) attached to iron oxide-coated quartz sand. Environ. Sci. Technol. 36 (11), 2403–2413.

Sadeghi, G., Schijven, J.F., Behrends, T., Hassanizadeh, S.M., Van Genuchten, M.T., 2013. Bacteriophage PRD1 batch experiments to study attachment, detachment and inactivation processes. J. Contaminant Hydrol. 152, 12–17.

Sasidharan, S., Bradford, S.A., Šimůnek, J., Torkzaban, S., Vanderzalm, J., 2017. Transport and fate of viruses in sediment and stormwater from a Managed Aquifer Recharge site. J. Hydrol. 555, 724–735.

Sasidharan, S., Bradford, S.A., Šimůnek, J., Torkzaban, S., 2018. Minimizing virus transport in porous media by optimizing solid phase inactivation. J. Environ. Qual. 47, 1058–1067. https://doi.org/10.2134/jeq2018.01.0027.

Schijven, J.F., Hoogenboezem, W., Hassanizadeh, M., Peters, J.H., 1999. Modeling removal of bacteriophages MS2 and PRD1 by dune recharge at Castricum, Netherlands. Water Resour. Res. 35 (4), 1101–1111.

Schijven, J.F., De Bruin, H.A.M., Hassanizadeh, S.M., de Roda Husman, A.M., 2003b. Bacteriophages and clostridium spores as indicator organisms for removal of pathogens by passage through saturated dune sand. Water Res. 37 (9), 2186–2194.

Schijven, J., Philip Berger, Ilkka Miettinen, 2003. Removal of pathogens, surrogates, indicators, and toxins using riverbank filtration. Riverbank Filtration. Springer Netherlands: 73–116.

Schijven J.F, Hassnizadeh S.M, Husman, A.M, 2010. Vulnerability of unconfined aquifers to virus contamination water research. 44, 4:1170–1181.

Schijven, J.F., Hassanizadeh, S.M., 2000. Removal of viruses by soil passage: overview of modeling, processes, and parameters. Crit. Rev. Environ. Sci. Technol. 30 (1), 49–127.

Schijven, J.F., Sadeghi, G., Hassanizadeh, S.M., 2016. Long-term inactivation of bacteriophage PRD1 as a function of temperature, pH, sodium and calcium concentration. Water Res. 103, 66–73.

Shen, C., et al., 2012. Theoretical and experimental investigation of detachment of colloids from rough collector surfaces. Colloids and Surfaces A: Physicochem. Eng. Aspects 410, 98–110. https://doi.org/10.1016/j.colsurfa.2012.06.025.

Sidhu, J.P.S., et al., 2015. Pathogen decay during managed aquifer recharge at four sites with different geochemical characteristics and recharge water sources. J. Environ. Quality 44 (5), 1402–1412. https://doi.org/10.2134/jeq2015.03.0118.

Sim, Y., Chrysikopoulos, C.V., 1996. One-dimensional virus transport in porous media with time dependent inactivation rate coefficients. Water Resour. Res. 32 (8), 2607–2611. https://doi.org/10.1029/96WR01496.

Šimůnek, J., Jarvis, N.J., Van Genuchten, M.T., Gärdenäs, A., 2003. Review and comparison of models for describing non-equilibrium and preferential flow and transport in the vadose zone. J. Hydrol. 272 (1), 14–35.

Simunek, J., van Genuchten, M.T., Sejna, M., 2016. Recent developments and applications of the HYDRUS computer software packages. Vadose Zone J. 15 (7), 25. https://doi.org/10.2136/vzj2016.04.0033.

Sinreich, M., Flynn, R., 2011. Comparative tracing experiments to investigate epikarst structural and compositional heterogeneity. Speleogenesis Evol. Karst Aquifers 10, 60–67.

Sudicky, E., MacQuarrie, K., 1989. Behaviour of biodegradable organic contaminants in random stationary hydraulic conductivity fields, Kobus, HE, and Kinzelbach, W., Contaminant Transport in Groundwater, International Symposium on Contaminant Transport in Groundwater, Stuttgart, pp. 307–315.

Torkzaban, S., Hassanizadeh, S.M., Schijven, J.F., De Bruin, H.A.M., De Roda Husman, A.M., 2006. Virus transport in saturated and unsaturated sand columns. Vadose Zone J. 5 (3), 877–885. https://doi.org/10.2136/vzj2005.0086.

Torkzaban, S., Bradford, S.A., Wan, J., Tokunaga, T., Masoudih, A., 2013. Release of quantum dot nanoparticles in porous media: role of cation exchange and aging time. Environ. Sci. Technol. 47 (20), 11528–11536. https://doi.org/10.1021/es402075f.

Torkzaban, S., Bradford, S.A., Vanderzalm, J.L., Patterson, B.M., Harris, B., Prommer, H., 2015. Colloid release and clogging in porous media: effects of solution ionic strength and flow velocity. J. Contam. Hydrol. 181, 161–171.

Tufenkji, N., Elimelech, M., 2004. Correlation equation for predicting single-collector efficiency in physicochemical filtration in saturated porous media. Environ. Sci. Technol. 38 (2), 529–536.

Unc, A., Goss, M.J., 2004. Transport of bacteria from manure and protection of water resources. Appl. Soil Ecol. 25 (1), 1–18. https://doi.org/10.1016/j.apsoil.2003.08.007.

Vadillo-Rodriguez, V., Busscher, H.J., Norde, W., de Vries, J., van der Mei, H.C., 2004. Atomic force microscopic corroboration of bond aging for adhesion of Streptococcus thermophilus to solid substrata. J. Colloid Interface Sci. 278 (1), 251–254. https://doi.org/10.1016/j.jcis.2004.05.045.

Wang, Y., Bradford, S.A., Šimůnek, J., 2014. Physicochemical factors influencing the preferential transport of in soils. Vadose Zone J. 13 (1). https://doi.org/10.2136/vzj2013.07.0120.

Xu, L.-C., Logan, B.E., 2006. Adhesion forces between functionalized latex microspheres and protein-coated surfaces evaluated using colloid probe atomic force microscopy. Colloids and Surfaces B: Biointerfaces 48 (1), 84–94.

Yao, K.-M., Habibian, M.T., O'Melia, C.R., 1971. Water and waste water filtration. Concepts and applications. Environ. Sci. Technol. 5 (11), 1105–1112. https://doi.org/10.1021/es60058a005.